Heat and Mass Transfer 36 (2000) 237–246 © Springer-Verlag 2000

Combined heat and mass transfer along a vertical moving cylinder with a free stream

H. S. Takhar, A. J. Chamkha, G. Nath

Abstract The mixed convection flow over a continuous moving vertical slender cylinder under the combined buoyancy effect of thermal and mass diffusion has been studied. Both uniform wall temperature (concentration) and uniform heat (mass) flux cases are included in the analysis. The problem is formulated in such a manner that when the ratio $\lambda(= u_w/(u_w + u_\infty)$, where u_w and u_∞ are the wall and free stream velocities, is zero, the problem reduces to the flow over a stationary cylinder, and when $\lambda = 1$ it reduces to the flow over a moving cylinder in an ambient fluid. The partial differential equations governing the flow have been solved numerically using an implicit finite-difference scheme. We have also obtained the solution using a perturbation technique with Shanks transformation. This transformation has been used to increase the range of the validity of the solution. For some particular cases closed form solutions are obtained. The surface skin friction, heat transfer and mass transfer increase with the buoyancy forces. The buoyancy forces cause considerable overshoot in the velocity profiles. The Prandtl number and the Schmidt number strongly affect the surface heat transfer and the mass transfer, respectively. The surface skin friction decreases as the relative velocity between the surface and free stream decreases.

1 Introduction

Mixed convection flow (combined forced and free convection flow) occurs in many industrial and technological applications which include nuclear reactors cooled during emergency shutdown, solar central receivers exposed to wind currents and heat exchangers placed in low-velocity environments. Mixed convection flows arise when the free stream, inertial and near-wall buoyant forces have strong effects on the resulting convecting heat transport. Flow over cylinders is considered to be two-dimensional if the body radius is large as compared to the boundary layer thickness. On the other hand, for slender cylinders the radius of the cylinder may be of the same order as the boundary layer thickness. Therefore, the flow may be considered as axisymmetric instead of two-dimensional. In this case, the governing equations contain the transverse curvature term which influences the velocity and temperature fields. The effect of the transverse curvature is important in certain applications such as wire and fibre drawing where accurate prediction is required and thick boundary layer can exist on slender or near slender bodies.

Mixed convection flow over a slender vertical cylinder due to the thermal diffusion has been considered by only a few investigators. Chen and Mucoglu [1] and Mucoglu and Chen [2] were the first to study this problem for the constant wall temperature [1] and the constant heat flux conditions [2]. They solved the partial differential equations approximately using the local non-similarity method [3–6]. Subsequently, Bui and Cebeci [7], Lee et al. [8, 9] and Wang and Kleinstruver [10] have solved this problem using an implicit finite-difference scheme.

There are several transport processes in industry and in nature where buoyancy forces arise from both thermal and mass diffusion caused by the temperature gradients and the concentration differences of dissimilar chemical species. Hence this analysis deals with the mixed convection boundary layer flow along a slender vertical heated cylinder which is moving with uniform velocity in the same direction as that of the free stream velocity. The buoyancy forces arise from both the thermal and mass diffusion processes. Both the uniform wall temperature (concentration) and the uniform heat (mass) flux cases are included in the analysis. The partial differential equations governing the flow, heat and mass transfer have been solved numerically using an implicit finite difference scheme [11]. We have also solved the governing equations by using the perturbation technique [12] which results in a system of ordinary differential equations. Further, we have used the Shanks transformation [13] to increase the range of the validity of the solution. For some particular cases, closed form solutions are also obtained. The results have been compared with those available in the literature [1, 2, 14].

2 Problem formulation

Let us consider the steady laminar incompressible mixed convection boundary layer flow along a heated vertical slender cylinder. Figure 1 gives the physical model and the coordinate system. The buoyancy forces arise from both the thermal and mass diffusion processes. The cylinder moves with uniform velocity in the same direction as that of the free stream velocity. The uniform wall temperature (concentration) as well as the uniform heat (mass) flux

Received on 17 May 1999

H. S. Takhar, A. J. Chamkha, G. Nath
The Manchester School of Engineering
The University of Manchester
Oxford Road
Manchester, M13 9PL, U.K.

Correspondence to: Dr. H. S. Takhar

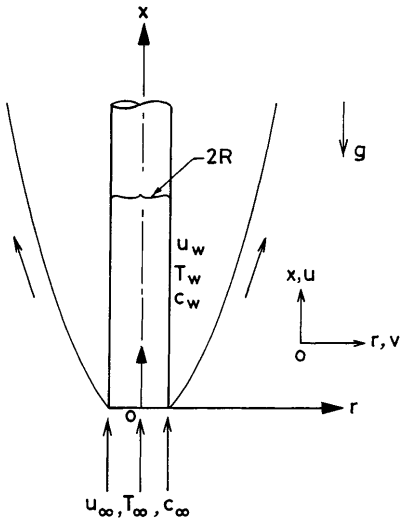

Fig. 1. Physical model and coordinate system

cases are considered. The free stream temperature and concentration are taken as constants. The analysis given here is confined to species diffusion procedures with very low concentration level such that the diffusion-thermo and the thermo-diffusion effects as well as the interfacial velocity at the wall due to species diffusion can be neglected. Under the foregoing assumptions and imposing the Boussinesq approximations, the boundary layer equations governing the flow, heat and mass transfer over a moving heated vertical slender cylinder can be expressed in the form [1, 2]

$$(ru)_x + (rv)_r = 0 \ , \tag{1}$$

$$uu_x + vu_r = (\nu/r)(ru_r)_r + g\beta(T - T_\infty) + g\beta^*(C - C_\infty) \ , \tag{2}$$

$$uT_x + vT_r = (\alpha/r)(rT_r)_r \ , \tag{3}$$

$$uC_x + vC_r = (D/r)(rC_r)_r \ . \tag{4}$$

The boundary conditions for both the uniform wall temperature and concentration (UWT/UWC), and the uniform heat and mass flux (UHF/UMF) are:

$$\begin{aligned} &r = R\text{: } u = u_w,\ v = 0,\ T = T_w,\\ &C = C_w,\ x \geq 0,\ \text{(for UWT/UWC)},\\ &r = R\text{: } u = u_w,\ v = 0,\ T_r = q_w/k,\\ &C_r = m_w/\rho D,\ x > 0,\ \text{(for UHF/UMF)},\\ &r \to \infty\text{: } u \to u_\infty,\ T \to T_\infty,\ C \to C_\infty,\ x \geq 0,\\ &x = 0\text{: } u = u_\infty,\ T = T_\infty,\ C = C_\infty,\ r > R \ . \end{aligned} \tag{5}$$

Here r is the distance measured from the axis of the cylinder in the radial direction; x is the distance measured along axial direction; u and v are the velocity components along the x and r directions, respectively; C and T are the concentration and the temperature of the fluid, respectively; g is the acceleration due to gravity; β and β^* are coefficient of thermal expansion and mass fraction expansion, respectively; α is the thermal diffusivity; D is binary diffusion coefficient; ν is the kinematic viscosity; q_w is the local surface heat-transfer rate per unit area; m_w is the mass flux of the diffusing species; R is the radius of the cylinder; k is the thermal conductivity; ρ is the density; the subscripts r and x denote derivative with respect to r and x, respectively; and the subscripts w and ∞ denote the conditions at the wall and in the free stream, respectively.

Uniform wall temperature/concentration (UWT/UWC)

In order to make Eqs. (1)–(4) dimensionless, we apply the following transformations

$$\begin{aligned} &\xi = (4/R)(vx/U)^{\frac{1}{2}},\ \eta = (U/vx)^{\frac{1}{2}}\left[(r^2 - R^2)/4R\right],\\ &U = u_w + u_\infty,\ \lambda = u_w/U\\ &u = \psi_r/r,\ v = -\psi_x/r;\ \psi = R(vUx)^{\frac{1}{2}} f(\xi,\eta),\\ &u = Uf'/2, \quad \theta(\xi,\eta) = (T - T_\infty)/(T_w - T_\infty);\\ &s(\xi,\eta) = (C - C_\infty)/(C_w - C_\infty),\ \mathrm{Pr} = \nu/\alpha,\\ &\mathrm{Sc} = \nu/D,\ \Omega = \mathrm{Gr}_t/\mathrm{Re}_x^2,\\ &\mathrm{Gr}_t = g\beta(T_w - T_\infty)x^3/\nu^2,\ \mathrm{Re}_x = Ux/\nu,\\ &N = \mathrm{Gr}_c/\mathrm{Gr}_t,\ \mathrm{Gr}_c = g\beta^*(C_w - C_\infty)x^3/\nu^2 \ , \end{aligned} \tag{6}$$

to Eqs. (1)–(4) and we find that Eq. (1) is identically satisfied and Eqs. (2)–(4) reduce to

$$(1 + \xi\eta)f''' + (f + \xi)f'' + 8\Omega(\theta + Ns) = \xi(f'f'_\xi - f''f_\xi) \ , \tag{7}$$

$$(1 + \xi\eta)\theta'' + (\mathrm{Pr}\, f + \xi)\theta' = \mathrm{Pr}\ \xi(f'\theta_\xi - \theta' f_\xi) \ , \tag{8}$$

$$(1 + \xi\eta)s'' + (\mathrm{Sc}\, f + \xi)s' = \mathrm{Sc}\ \xi(f's_\xi - s'f_\xi) \ . \tag{9}$$

The boundary conditions are

$$\begin{aligned} &f(\xi,0) = 0,\ f'(\xi,0) = 2\lambda,\ \theta(\xi,0) = s(\xi,0) = 1,\\ &f'(\xi,\infty) = 2(1 - \lambda),\ \theta(\xi,\infty) = s(\xi,\infty) = 0 \ . \end{aligned} \tag{10}$$

Here ξ and η are the transformed coordinates and ξ also represents the curvature parameter; f and ψ are, respectively, dimensionless and dimensional stream functions; f' is the dimensionless velocity; θ and s are, respectively dimensionless temperature and concentration; U is the composite velocity; Gr_t and Gr_c are Grashof numbers for thermal and mass diffusion, respectively Re_x is the Reynolds number; Ω is the buoyancy parameter due to thermal diffusion; λ is the ratio of the wall velocity to the composite velocity; Pr and Sc are the Prandtl number and Schmidt number, respectively; N is a measure of the relative effects between buoyancy forces that arise from mass diffusion and thermal diffusion and for $N > 0$ the buoyancy force due to concentration difference assists the thermal buoyancy force; the subscripts ξ denotes derivative with respect to ξ; and prime denotes derivative with respect to η.

The surface skin friction coefficient C_f, the surface heat transfer coefficient in terms of the Nusselt number Nu, and the surface mass transfer coefficient in terms of the Sherwood number Sh are expressed as:

$$\begin{aligned} &C_f = 2\mu(\partial u/\partial r)_{r=R} = R/\rho U^2 = 2^{-1}(\mathrm{Re}_x)^{-1/2} f''(\xi,0),\\ &\mathrm{Nu} = -x(\partial T/\partial r)_{r=R}/(T_w - T_\infty)\\ &\quad = -2^{-1}(\mathrm{Re}_x)^{1/2}\theta'(\xi,0), \end{aligned}$$

$$\mathrm{Sh} = -x(\partial C/\partial r)_{r=R}/(C_w - C_\infty) = -2^{-1}(\mathrm{Re}_x)^{1/2} s'(\xi, 0) \ . \tag{11}$$

Uniform heat/mass flux (UHF/UMF)

For this case, we use the following transformations

$$\xi = (4/R)(vx/U)^{1/2}, \quad \eta = (U/vx)^{1/2}\left[(r^2 - R^2)/4R\right],$$
$$\psi(x, y) = R(vUx)^{1/2} F(\xi, \eta),$$
$$\phi(\xi, \eta) = (\mathrm{Re}_x)^{1/2}(T - T_\infty)/(q_w x/k), \tag{12}$$
$$S(\xi, \eta) = (\mathrm{Re}_x)^{1/2}(C - C_\infty)/(m_w x/\rho D),$$
$$\Omega^* = \mathrm{Gr}_t^*/(\mathrm{Re}_x)^{5/2}, \quad \mathrm{Gr}_t^* = g\beta q_w x^4/(kv^2),$$
$$N^* = \mathrm{Gr}_c^*/\mathrm{Gr}_t^*, \quad \mathrm{Gr}_c^* = g\beta^* m_w x^4/(\rho D v^2) \ .$$

The other notations are the same as in (6). The above transformations are applied to Eqs. (1)–(4) and we find that (1) is identically satisfied and (2)–(4) reduce to

$$(1 + \xi\eta)F''' + (F + \xi)F'' + 8\Omega^*(\phi + N^* S) = \xi(F' F'_\xi - F'' F_\xi) \ , \tag{13}$$
$$(1 + \xi\eta)\phi'' + (\mathrm{Pr}\, F + \xi)\phi' - \mathrm{Pr}\, F'\phi = \mathrm{Pr}\, \xi(F'\phi_\xi - \phi' F_\xi) \ , \tag{14}$$
$$(1 + \xi\eta)S'' + (\mathrm{Sc}\, F + \xi)S' - \mathrm{Sc}\, F' S = \mathrm{Sc}\, \xi(F' S_\xi - S' F_\xi) \ . \tag{15}$$

The boundary conditions are given by:

$$F(\xi,0) = 0,\ F'(\xi,0) = 2\lambda,\ \phi'(\xi,0) = S'(\xi,0) = -2,\quad F'(\xi,0) = 2(1-\lambda),\ \phi(\xi,\infty) = S(\xi,\infty) = 0 \ . \tag{16}$$

Here F is the dimensionless stream function; F' is the dimensionless velocity; ϕ and S are the dimensionless temperature and concentration, respectively; Ω^* is the buoyancy parameter due to the thermal diffusion; N^* measures the relative effects of buoyancy forces that arise due to mass diffusion and thermal diffusion; Gr_t^* and Gr_c^* are the Grashof numbers due to the thermal and mass diffusion, respectively; μ is the dynamic viscosity and all other notations are the same as those in the (UWT/UWC) case.

The skin friction coefficient C_f^*, the heat transfer coefficient Nu^* and the mass transfer coefficient Sh^* can be expressed as

$$C_f^* = 2\mu(\partial u/\partial r)_{r=R}/\rho U^2 = 2^{-1}(\mathrm{Re}_x)^{-1/2} F''(\xi, 0),$$
$$\mathrm{Nu}^* = q_w x/[k(T_w - T_\infty)] = (\mathrm{Re}_x)^{1/2}[\phi(\xi,0)]^{-1}, \tag{17}$$
$$\mathrm{Sh}^* = m_w x/[\rho D(C_w - C_\infty)] = (\mathrm{Re}_x)^{1/2}[S(\xi,0)]^{-1} \ .$$

It may be remarked that Eqs. (7) and (8), and Eqs. (13) and (14) for $\lambda = N = N^* = 0$ are identical to those of Chen and Mucoglu [1], and Mucoglu and Chen [2], respectively. Also, for $\lambda = 1/2$, $\Omega = 0$ Eqs. (7) and (8) are the same as those of Karnis and Pechoc [14].

3 Numerical method

The partial differential Eqs. (7)–(9) under the boundary conditions (10) and Eqs. (13)–(15) under the boundary conditions (16) were solved numerically by an implicit, iterative tridiagonal finite-difference method similar to that discussed by Blottner [11]. All the first-order derivatives with respect to ξ are replaced by two-point backward difference formulae of the form

$$\partial B/\partial\xi = (B_{i,j} - B_{i-1,j})/\Delta\xi \tag{18}$$

where B is any dependent variable and i and j are the node locations along the ξ and η directions, respectively. First the third-order differential Eqs. (7) and (13) are converted into second order by substituting $f' = h$ and $F' = H$, respectively. Then the second-order differential equations for h, θ, s, H, ϕ and S are discretized using three-point central difference formulae while all first-order differential equations are discretized by employing the trapezoidal rule. At each line of constant ξ, a system of algebraic equations is obtained. With the nonlinear terms evaluated at the previous iteration, the algebraic equations are solved iteratively by using the well known Thomas algorithm [11]. The same process is repeated for the next ξ value and the equations are solved line by line until the desired ξ value is reached. A convergence criterion based on the relative difference between the current and the previous iterations is employed. When this difference reaches 10^{-5}, the solution is assumed to have converged and the iterative process is terminated.

The effect of the grid size $\Delta\eta$ and $\Delta\xi$ and the edge of the boundary layer η_∞ on the solutions is also examined. The results presented here are independent of the grid size and η_∞ at least up to the 4th decimal place.

4 Perturbation method

It is also possible to solve Eqs. (7)–(9) under the boundary conditions (10) and Eqs. (13)–(15) under the boundary conditions (16) by a perturbation expansion procedure [12] in terms of the axial distance ξ. This approximate method is valid for small values of ξ. However, by using the Shanks transformation [13], the range of validity of ξ can be increased. This method gives good results and we have to solve a system of ordinary differential equations instead of the partial differential equations. First we solve Eqs. (7)–(9) under the boundary conditions (10) and assume a regular perturbation expansion for f; θ and s in powers of ξ as

$$f(\xi, \eta) = \sum_{n=0}^{\infty} \xi^n f_n(\eta), \quad \theta(\xi, \eta) = \sum_{n=0}^{\infty} \xi^n \theta_n(\eta), \quad s(\xi, \eta) = \sum_{n=0}^{\infty} \xi^n s_n(\eta) \tag{19}$$

Substituting (19) into Eqs. (7)–(10) and equating coefficients of like powers of ξ and truncating the expansion at the nth term, we obtain for $n = 0$.

$$f_0''' f_0 f_0'' + 8\Omega(\theta_0 + N s_0) = 0 \ , \tag{20a}$$

$$\theta_0'' + \mathrm{Pr} f_0 \theta_0' = 0 \ , \tag{20b}$$

$$s_0'' + \mathrm{Sc} f_0 s_0' = 0 \ , \tag{20c}$$

$$f_0(0) = 0, \quad f_0'(0) = 2\lambda, \quad \theta_0(0) = s_0(0) = 1,$$
$$f_0'(\infty) = 2(1-\lambda), \quad \theta_0(\infty) = s_0(\infty) = 0 \ . \tag{20d}$$

and for $n \geq 1$

$$f''' + \sum_{m=0}^{n} f_m f''_{n-m} + 8\Omega(\theta_n + N s_n)$$
$$= \sum_{m=0}^{n-1} (n-m)(f_m' f'_{n-m-1} - f_m'' f_{n-m-1}) - \eta f''' - f''_{n-1} \ , \tag{21a}$$

$$\theta'' + \mathrm{Pr} \sum_{m=0}^{n} f_m \theta'_{n-m}$$
$$= \mathrm{Pr} \sum_{m=0}^{n-1} (n-m)(f_m' \theta_{n-m-1} - \theta_m' f_{n-m-1}) - \eta \theta''_{n-1} - \theta'_{n-1} \ , \tag{21b}$$

$$s'' + \mathrm{Sc} \sum_{m=0}^{n} f_m s'_{n-m}$$
$$= \mathrm{Sc} \sum_{m=0}^{n-1} (n-m)(f_m' s_{n-m-1} - s_m' f_{n-m-1}) - \eta s''_{n-1} - s'_{n-1} \ , \tag{21c}$$

$$f_n = f_n' = \theta_n = s_n = 0 \text{ at } \eta = 0,$$
$$f_n' = \theta_n = s_n \to 0 \text{ as } n \to \infty \ . \tag{21d}$$

Also we have

$$f''(\xi, 0) = \sum_{n=0}^{\infty} \xi^n f_n''(0), \ \theta'(\xi, 0) = \sum_{n=0}^{\infty} \xi^n \theta_n(0),$$
$$s'(\xi, 0) = \sum_{n=0}^{\infty} \xi^n s_n'(0) \ . \tag{22}$$

Using a perturbation expansion for F, ϕ and S similar to that given in (19) and following the above procedure in Eqs. (13)–(16), we get for $n = 0$

$$F_0''' + F_0 F_0'' + 8\Omega^*(\phi_0 + N^* S_0) = 0 \tag{23a}$$

$$\phi_0'' + \mathrm{Pr}\,(F_0 \phi_0' - F_0' \phi_0) = 0 \ . \tag{23b}$$

$$S_0'' + \mathrm{Sc}\,(F_0 S_0' - F_0' S_0) = 0 \tag{23c}$$

$$F_0 = 0, \ F_0' = 2\lambda, \ \phi_0' = S_0' = -2 \text{ at } \eta = 0,$$
$$F_0 = 2(1-\lambda), \ \phi_0 = S_0 = 0 \text{ as } \eta \to \infty \ . \tag{23d}$$

and for $n \geq 1$.

$$F''' + \sum_{m=0}^{n} F_m F''_{n-m} + 8\Omega^*(\phi_n + N S_n)$$
$$= \sum_{m=0}^{n-1} (n-m)(F_m' F''_{n-m-1}) - \eta F'''_{n-1} - F''_{n-1} \ , \tag{24a}$$

$$\phi'' + \mathrm{Pr} \sum_{m=0}^{n} (F_m \phi'_{n-m} - F_m' \phi_{n-m}) =$$
$$\mathrm{Pr} \sum_{m=0}^{n-1} (n-m)(F'_{n-m-1} - \phi_m' F_{n-m-1}) - \eta \phi''_{n-1} - \phi'_{n-1} \ , \tag{24b}$$

$$S'' + \mathrm{Sc} \sum_{m=0}^{n} (F_m S'_{n-m} - F_m' S_{n-m}) =$$
$$\mathrm{Sc} \sum_{m=0}^{n-1} (n-m)(F_m' S_{n-m-1} - S_m' F_{n-m-1}) - \eta S''_{n-1} - S'_{n-1} \ , \tag{24c}$$

$$F_n = F_n' = \phi_n' = S_n' = 0 \text{ at } \eta = 0 \ ,$$
$$F_n' = \phi_n = S_n \to 0 \text{ as } \eta \to \infty \ . \tag{24d}$$

Further, we get

$$F''(\xi, 0) = \sum_{n=0}^{\infty} \xi^n F_n''(0); \ \phi(\xi, 0) = \sum_{n=0}^{\infty} \xi^n \phi_n(0),$$
$$S(\xi, 0) = \sum_{n=0}^{\infty} \xi^n S_n(0) \ . \tag{25}$$

Equations (20a)–(20c) and (23a)–(23c) are non-linear equations and they are solved by using the shooting method [15]. Equations (21a)–(21c) and (24a)–(24c) are linear equations which are solved by the method of superposition [15].

As mentioned earlier, the perturbation method is valid for small values of ξ. However, its range of validity can be enhanced by using the Shanks transformation [13]. Since we are mainly interested in surface skin friction, heat transfer and mass transfer coefficients given in Eqs. (11) and (17) for (UWT/UWC) and (UHF/UMF) cases, respectively, we apply the Shanks transformation

$$e(L_n) = (L_{n+1} L_{n-1} - L_n^2)/(L_{n+1} + L_{n-1} - 2L_n) \tag{26}$$

to Eqs. (22) and (25). Here e is the operator and L_n denotes the partial sum of the series. For our case we taken $n = 4$ and apply the above transformation twice and we find that the results are in excellent agreement with the numerical results in the range $0 \leq \xi \leq 1$. The maximum difference is less than 0.5%.

5
Analytical solution

Equation (7) under the boundary conditions on f given in (10) for $\Omega = 0$, $\lambda = 0.5$ admits a closed form solution given by

$$f(\xi, \eta) = \eta \ . \tag{27a}$$

Using (27a), Eqs. (8) and (9) under the boundary conditions (10) for $\Omega = \xi = 0$, $\lambda = 0.5$ also admit closed form solutions given by

$$\theta(\eta) = \mathrm{erfc}\left[(\mathrm{Pr}/2)^{1/2} \eta\right] \ , \tag{27b}$$

$$s(\eta) = \mathrm{erfc}\left[(\mathrm{Sc}/2)^{1/2} \eta\right] \ . \tag{27c}$$

Similarly, Eq. (13) for $\Omega^* = 0$, $\lambda = 0.5$ and Eqs. (14) and (15) for $\Omega^* = \xi = 0$, $\lambda = 0.5$ under the conditions (16) also have closed form solution [16], given by;

$$F(\xi, \eta) = \eta \tag{28a}$$

$$\phi(\eta) = -2\exp(-\mathrm{Pr}\,\eta^2/2)\left[\left(\frac{A_1}{A_2}\right)|F|\left(\frac{\mathrm{Pr}+3}{4}, \frac{1}{2}, \frac{\mathrm{Pr}\,\eta^2}{4}\right) + \eta|F|\left(\frac{\mathrm{Pr}+5}{4}, \frac{3}{2}, \frac{\mathrm{Pr}\,\eta^2}{4}\right)\right], \tag{28b}$$

$$S(\eta) = -2\exp(-\mathrm{Sc}\,\eta^2/2)\left[\left(\frac{A_3}{A_4}\right)|F|\left(\frac{\mathrm{Sc}+3}{4}, \frac{1}{2}, \frac{\mathrm{Sc}\,\eta^2}{4}\right) + \eta|F|\left(\frac{\mathrm{Sc}+5}{4}, \frac{3}{2}, \frac{\mathrm{Sc}\,\eta^2}{4}\right)\right] \tag{28c}$$

where

$$A_1 = \Gamma\left(\frac{1}{2}\right)\Big/\Gamma\left(\frac{\mathrm{Pr}+5}{4}\right),$$

$$A_2 = 2^{-1/2}\Gamma(-1/2)/\Gamma\left(\frac{\mathrm{Pr}+3}{4}\right), \tag{28d}$$

$$A_3 = \Gamma(1/2)/\Gamma\left(\frac{\mathrm{Sc}+5}{4}\right),$$

$$A_4 = 2^{-1/2}\Gamma(-1/2)/\Gamma\left(\frac{\mathrm{Sc}+3}{4}\right). \tag{28e}$$

Here $|F|(\ )$ is the confluent hypergeometric function and $\Gamma(\ )$ is the gamma function. The surface skin friction, heat transfer and mass transfer for both the (UWT/UWC) and the (UHF/UMF) are found to be identical to those of the numerical solution up to the 4th decimal place.

6 Results and discussion

In order to assess the accuracy of our method, we have compared the surface skin friction $(f''(\xi, 0))$, and the surface heat transfer $(-\theta'(\xi, 0))$ for $\lambda = 0$ (stationary wall) and $N = \mathrm{O}$ (no mass diffusion), when the wall temperature is uniform, with those of Chen and Mucoglu [1]. The corresponding results for the uniform heat flux case are compared with those of Mucoglu and Chen [2]. We have also compared the surface heat transfer $(\mathrm{Nu}\ (\mathrm{Re}_x)^{-1/2})$ for $\Omega = 0$ (without buoyancy forces), $\lambda = 0.5$ (moving wall) and for uniform wall temperature case with those of Karnis and Pechoc [14]. The results are found to be in good agreement. The comparison is presented in Tables 1–3.

The effect of surface curvature parameter ξ (or the axial distance) on the velocity, temperature and concentration profiles (f', θ, s) for $\Omega = 1$, $N = \lambda = 0.5$, Pr = 0.71, Sc = 0.9 are given in Figs. 2–4. The velocity, thermal and concentration boundary layers increase due to the curvature ξ. Similar trend has been observed by Chen and Mucoglu [1] for $\lambda = N = 0$. The interesting result is that the velocity profiles near the wall, in the presence of buoyancy force which assists the motion $(\Omega > 0)$, exceed the velocity at the edge of the boundary layer (i.e., there is an overshoot in the velocity f') and the magnitude of the velocity overshoot slightly decreases as the curvature increases. The velocity overshoot is about 150% and it

Table 1. Comparison of skin friction and heat transfer results $(f''(\xi, 0), -\theta'(\xi, 0))$ for uniform wall temperature case when $N = \lambda = 0$, Pr = 0.7

ξ	Ω	Present results		Chen and Mucoglu [1]	
		$f''(\xi, 0)$	$-\theta'(\xi, 0)$	$f''(\xi, 0)$	$-\theta(\xi, 0)$
0	0	1.3281	0.5854	1.3282	0.5854
0	1	4.9663	0.8219	4.9668	0.8221
0	2	7.7119	0.9302	7.7126	0.9305
1	0	1.9167	0.8666	1.9172	0.8669
1	1	5.2578	1.0617	5.2584	1.0621
1	2	7.8863	1.1685	7.8871	1.1690
2	0	2.3975	1.0963	2.3981	1.0968
2	1	5.6993	1.2712	5.7001	1.2718
2	2	8.3555	1.3741	3.3566	1.3747

Table 2. Comparison of skin friction $(f''(\xi, 0))$ and the reciprocal of heat transfer $(\phi(\xi, 0))$ for uniform heat flux case when $N = \lambda = 0$, Pr = 0.7

ξ	Ω^*	Present results		Mucoglu and Chen [2]	
		$F''(\xi, 0)$	$\phi(\xi, 0)$	$F''(\xi, 0)$	$\phi(\xi, 0)$
0	0	1.3281	2.4636	1.3282	2.4637
0	1.0	6.3659	1.7922	6.3665	1.7923
0	1.5	8.0157	1.6908	8.0165	1.6911
1	0	1.9108	1.8539	1.9113	1.8543
1	1.0	5.9407	1.4701	5.9414	1.4705
1	1.5	7.3443	1.3965	7.3451	1.3970
2	0	2.3840	1.5337	2.3847	1.5343
2	1.0	5.9312	1.3001	5.9322	1.3007
2	1.5	7.2546	1.2450	7.2558	1.2458

Table 3. Comparison of heat transfer results $(\mathrm{Nu}(\mathrm{Re}_x)^{-1/2})$ for the uniform wall temperature case when $\Omega = 0$, $\lambda = 0.5$

ξ	Present results		Karnis and Pechoc [14]	
	Pr = 0.7	Pr = 1.0	Pr = 0.7	Pr = 1.0
0.0001	0.35144	0.44411	0.35288	0.44754
0.001	0.35434	0.44761	0.36070	0.45570
0.005	0.36261	0.45613	0.37467	0.47026
0.01	0.37054	0.46427	0.38499	0.48103
0.04	0.40504	0.49895	0.41930	0.51682
0.05	0.41443	0.50817	0.42719	0.52506
0.06	0.42328	0.51667	0.43425	0.53243

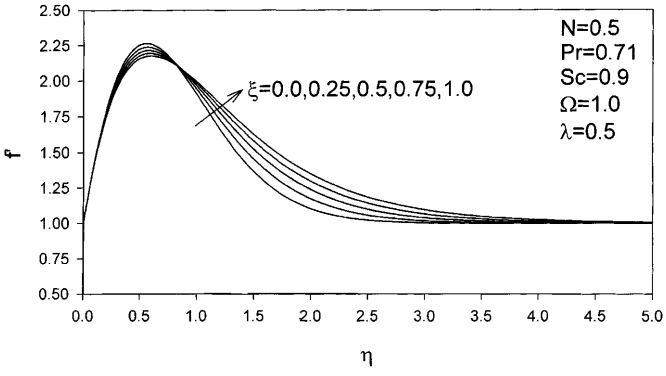

Fig. 2. Effect of ξ on velocity profiles (UWT/UWC)

decreases by about 5% as ξ increases from zero to 1. Chen and Mucoglu [1] have observed a similar trend. The reason for the velocity overshoot is that the buoyancy force ($\Omega > 0$) acts like a favourable pressure gradient which imparts additional momentum in the boundary layer and thus causing an increase in the velocity beyond its edge values. As the curvature increases the boundary layer thickness overshoot in the velocity is reduced.

Figures 5–7 show the effect of the Prandtl number Pr on the surface skin friction coefficient ($2\mathrm{Re}_x^{1/2} C_f = f''(\xi, 0)$), the Nusselt number ($2\mathrm{Re}_x^{1/2}\mathrm{Nu} = -\theta'(\xi, 0)$) and the Sherwood number ($2\mathrm{Re}_x^{-1/2}\mathrm{Sh} = -s'(\xi, 0)$). The surface heat transfer ($-\theta'(\xi, 0)$) increases with Pr for all ξ, because the thermal boundary layer becomes thin with increasing

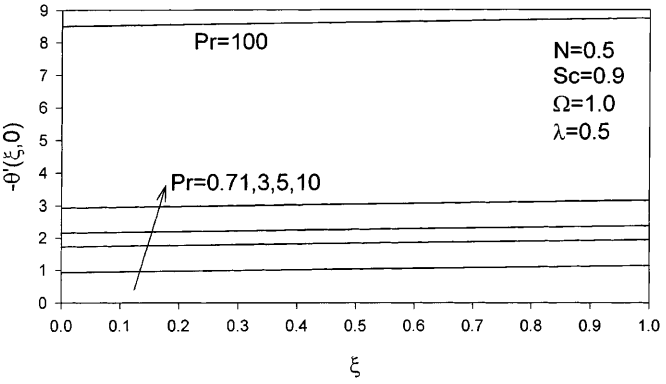

Fig. 6. Effect of Pr on the heat transfer (UWT/UWC)

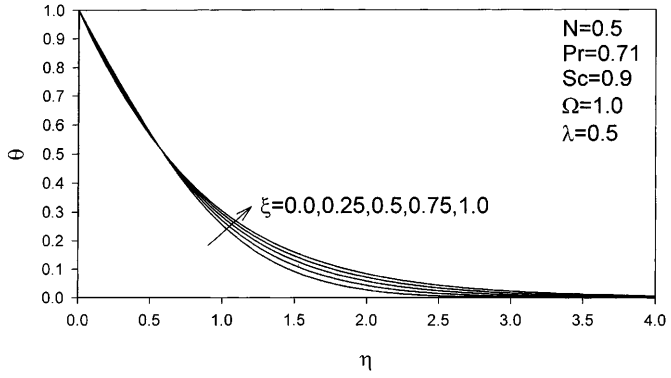

Fig. 3. Effect of ξ on temperature profiles (UWT/UWC)

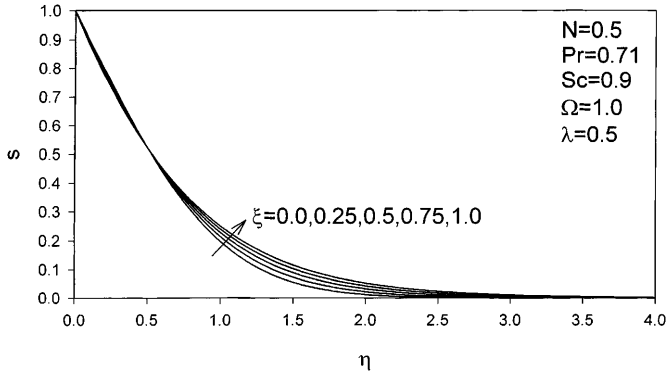

Fig. 4. Effect of ξ on concentration profiles (UWT/UWC)

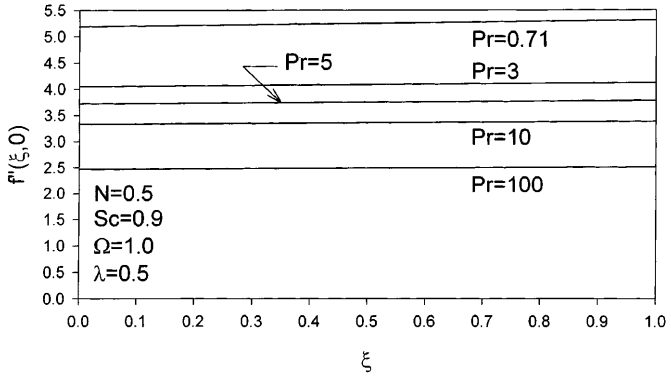

Fig. 5. Effect of Pr on the skin friction (UWT/UWC)

Pr. This reduces the temperature and increases the temperature gradient. Since higher Pr implies more viscous fluid, the velocity and concentration boundary layers grow with increasing Pr. This causes a reduction in the surface skin friction ($f''(\xi, 0)$) and the mass transfer ($-s'(\xi, 0)$). However, the effect of Pr is found to be more pronounced on the surface heat transfer ($-\theta'(\xi, 0)$) than on the surface skin friction ($f''(\xi, 0)$) and the surface mass transfer ($-s'(\xi, 0)$). For example, for $\Omega = 1$, $\lambda = N = 0.5$, Sc = 0.9, $\xi = 1$, the heat transfer ($-\theta'(\xi, 0)$) increases by about 300% as Pr increases from 0.71 to 10, whereas the surface skin friction ($f''(\xi, 0)$) and the surface mass transfer ($-s'(\xi, 0)$) decrease by about 37% and about 10%, respectively. The strong dependence of $-\theta'(\xi, 0)$ on Pr is because Pr occurs in the energy equation, whereas the effect of Pr on $f''(\xi, 0)$, and $-s'(\xi, 0)$ is only indirect.

Figures 8–10 display the effect of Schmidt number (Sc) on the surface skin friction, heat transfer and mass transfer ($f''(\xi, 0)$, $-\theta'(\xi, 0)$, $-s'(\xi, 0)$). The effect is qualitatively similar to that of Pr. The mass transfer ($-s'(\xi, 0)$) is strongly affected by Sc due to its presence in the diffusion equation, whereas the effect of Sc on the skin friction ($f'(\xi, 0)$) and the heat transfer ($-\theta'(\xi, 0)$) is comparatively weak. For $\Omega = 1$, $\lambda = N = 0.5$, Pr = 0.71, $\xi = 1$, $-s'(\xi, 0)$ increases by about 180% as Sc increases from 0.1 to 1.3. On the other hand, $f''(\xi, 0)$ and $-\theta'(\xi, 0)$ decrease by about 20% and 7.5%, respectively.

In Figs. 11–13, the effect of λ on the surface skin friction ($f''(\xi, 0)$), heat transfer ($-\theta'(\xi, 0)$) and mass transfer ($-s'(\xi, 0)$) for $N = 0.5$, $\Omega = 1$, Pr = 0.71, Sc = 0.9 is

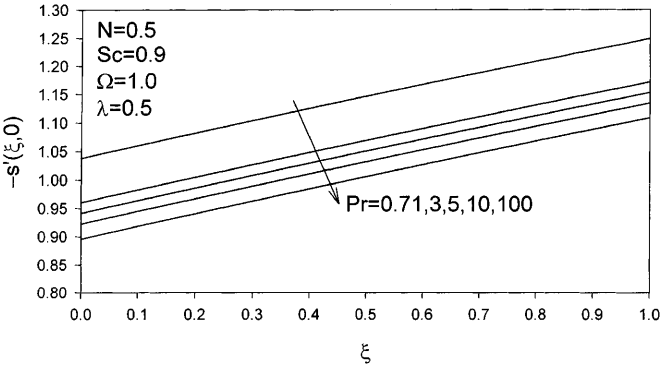

Fig. 7. Effect of Pr on the mass transfer (UWT/UWC)

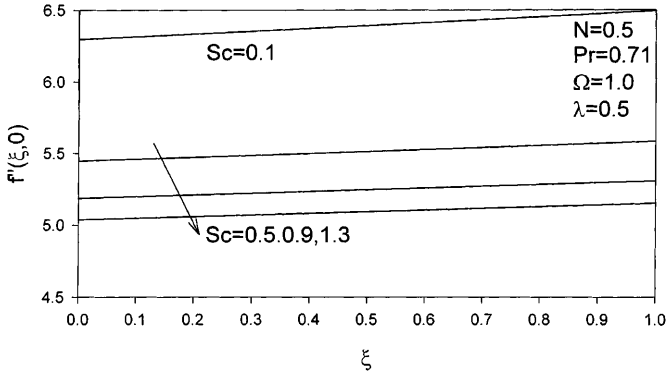

Fig. 8. Effect of Sc on the skin friction (UWT/UWC)

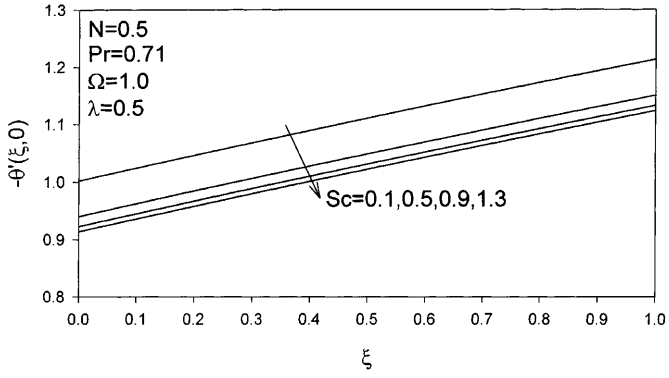

Fig. 9. Effect of Sc on the heat transfer (UWT/UWC)

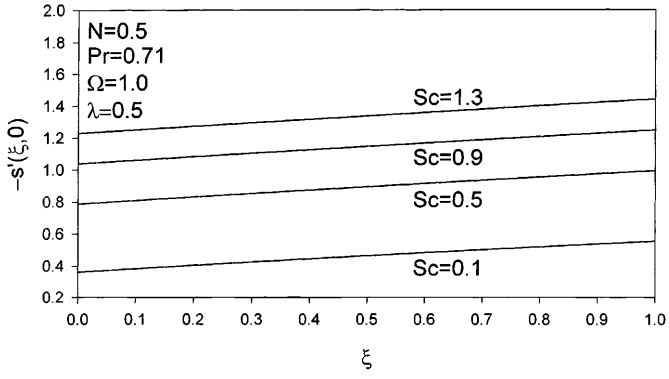

Fig. 10. Effect of Sc on the mass transfer (UWT/UWC)

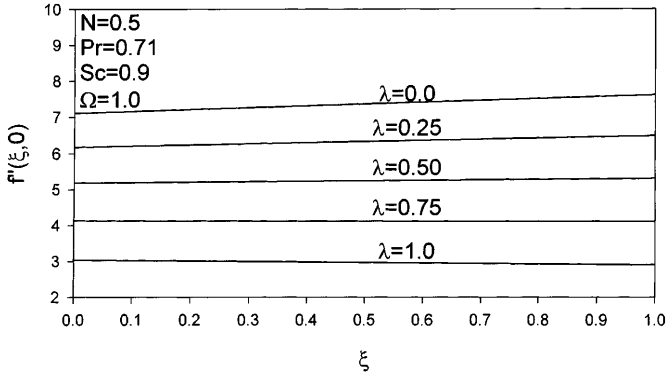

Fig. 11. Effect of λ on the skin friction (UWT/UWC)

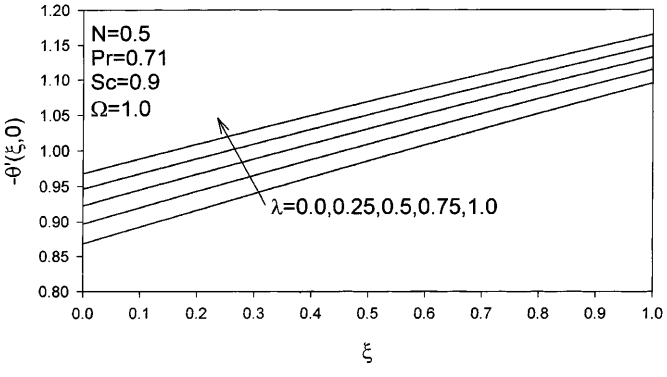

Fig. 12. Effect of λ on the heat transfer (UWT/UWC)

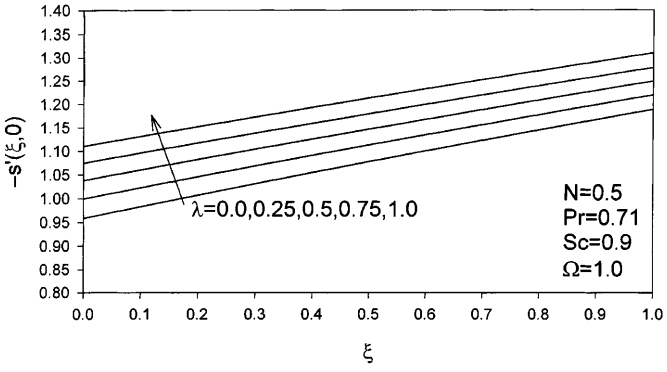

Fig. 13. Effect of λ on the mass transfer (UWT/UWC)

displayed. The surface skin friction $f''(\xi,0)$ decreases with increasing λ, because an increase in λ implies reduction in the relative velocity between wall and free stream. This causes the momentum boundary layer to become thick which results in a reduction in the surface skin friction. On the other hand, the surface heat and mass transfer $(\theta'(\xi,0), -s'(\xi,0)$ increase with λ. This is because at low Prandtl number (Pr) or Schmidt number (Sc), the thermal or concentration boundary layer is thicker than the momentum boundary layer. Hence the thermal or concentration boundary layer depends on the flow outside the momentum boundary layer. Hence at low Pr or Sc, the heat and mass transfer increase with λ. For $\Omega = 1$, $N = 0.5$, Pr = 0.71, Sc = 0.9, $\xi = 1$, the surface skin friction decreases by about 57% as λ increases from 0 to 1, but the surface heat and mass transfer increase by about 10%.

The effect of the parameter, N, which measures the relative magnitude of the buoyancy forces due to the mass diffusion and thermal diffusion, on the skin friction $(f''(\xi,0))$ and heat and mass transfer $(-\theta'(\xi,0) - s'(\xi,0))$ is shown in Figs. 14–16. The skin friction $(f''(\xi,0))$, and heat and mass transfer $(-\theta'(\xi,0) - s'(\xi,0))$ increase, respectively, by about 200, 20 and 21% as N increases form 0 to 3. The reason for a significant increase in the skin friction is that N occurs in the momentum equation and the effect of N on heat and mass transfer is indirect. Also increasing $N\,(N > 0)$ implies an increase in the buoyancy forces which behave like favourable pressure gradient when $\Omega > 0$.

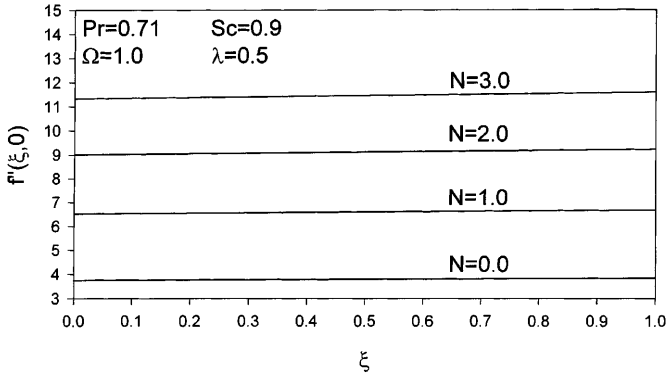

Fig. 14. Effect of N on the skin friction (UWT/UWC)

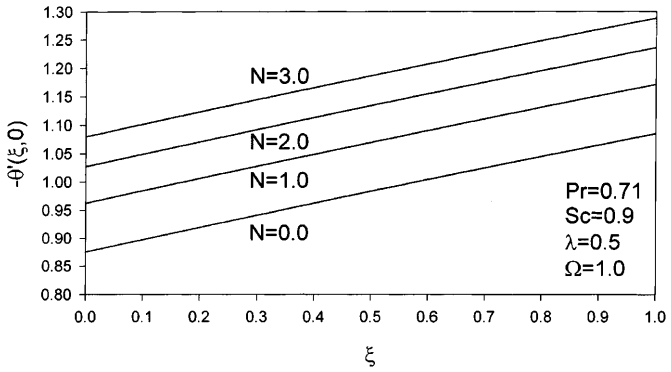

Fig. 15. Effect of N on the heat transfer (UWT/UWC)

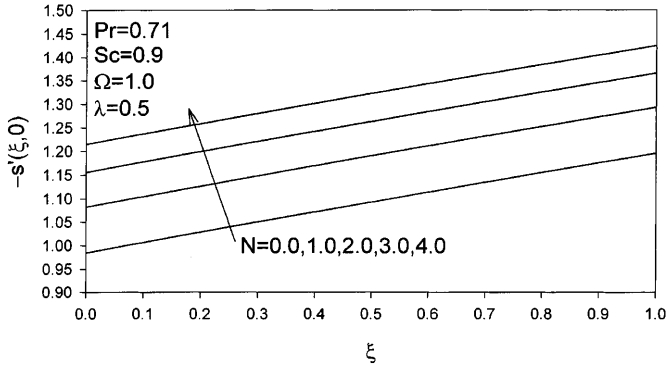

Fig. 16. Effect of N on the mass transfer (UWT/UWC)

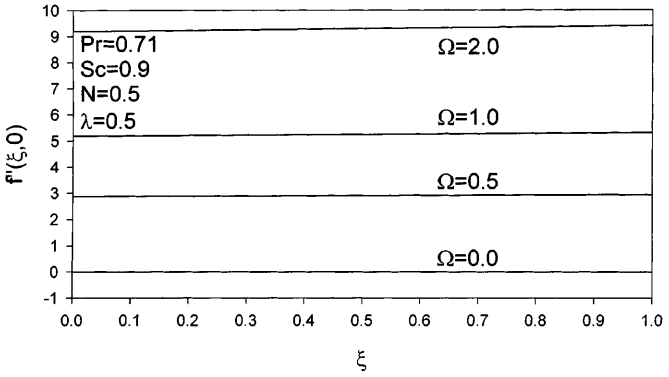

Fig. 17. Effect of Ω on the skin friction (UWT/UWC)

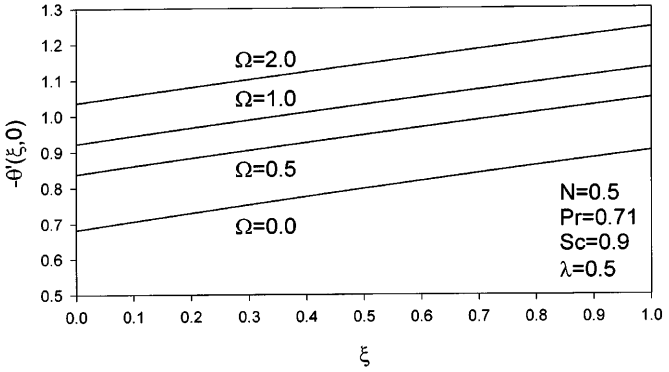

Fig. 18. Effect of Ω on the heat transfer (UWT/UWC)

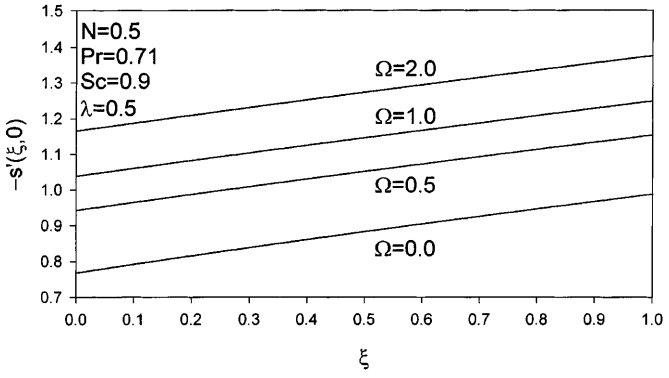

Fig. 19. Effect of Ω on the mass transfer (UWT/UWC)

The effect of the buoyancy parameter Ω on the surface skin friction, heat transfer and mass transfer $(f''(\xi,0), -\theta'(\xi,0) - s'(\xi,0))$ is presented in Figs. 17–19. Since an increase in Ω implies increase in the favourable pressure gradient which accelerates the motion and reduces the boundary layer thickness, the skin friction, heat transfer and mass transfer are enhanced. The surface skin friction, heat transfer and mass transfer for $N = \lambda = 0.5$, $\xi = 1$, Pr = 0.71, Sc = 0.9 increase by about 217, 20, 20%, respectively, as Ω increases from 0.5 to 2. The reason for the strong dependence of th skin friction on Ω is that it occurs only in the momentum equation. The effect of the curvature parameter ξ on $f''(\xi,0)$ is found to be small.

The effect of the curvature ξ on the velocity, temperature and concentration profiles (F, ϕ, S) for $\Omega = 1$, $N = \lambda = 0.5$, Pr = 0.71, Sc = 0.9 and for uniform heat (mass) flux (UHF/UMF) is displayed in Figs. 20–22. Since the effect is qualitatively similar to that for the uniform wall temperature (concentration) case, it is not discussed here.

Figures 23–25 show the effect of the wall velocity λ on the skin friction $(F''(\xi,0))$, heat transfer $(1/\phi(\xi,0))$ and mass transfer $(1/S(\xi,0))$ for the (UHF/UMF) case when $\Omega = 1$, $N = \lambda = 0.5$, Pr = 0.71, Sc = 0.9. The skin friction decreases by about 61% when λ increases form zero to 1, whereas the heat and mass transfer increase, respectively, by about 21% and 31%. The effect of λ is qualitatively

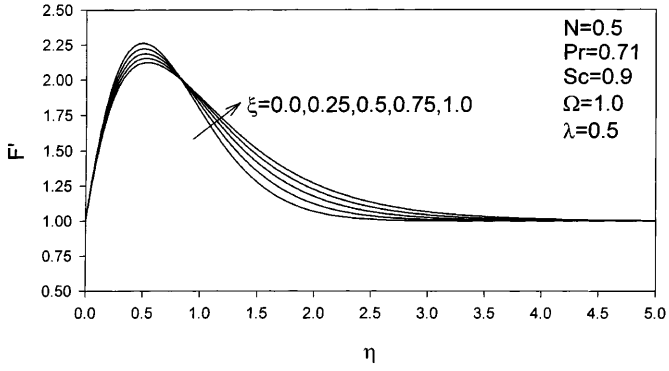

Fig. 20. Effect of ξ on the velocity profiles (UHF/UMF)

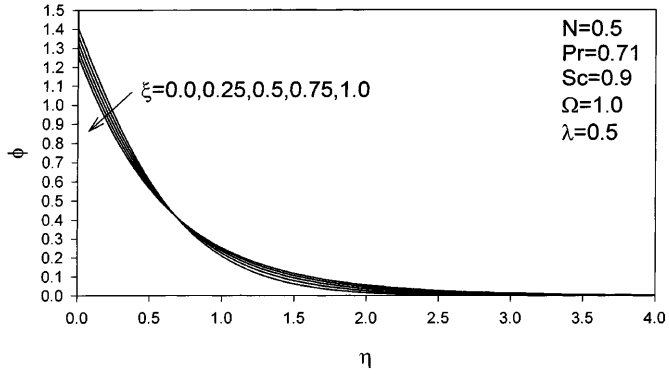

Fig. 21. Effect of ξ on temperature profiles (UHF/UMF)

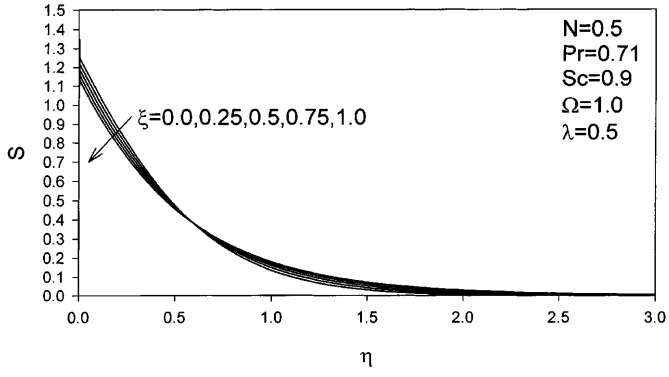

Fig. 22. Effect of ξ on concentration profiles (UHF/UMF)

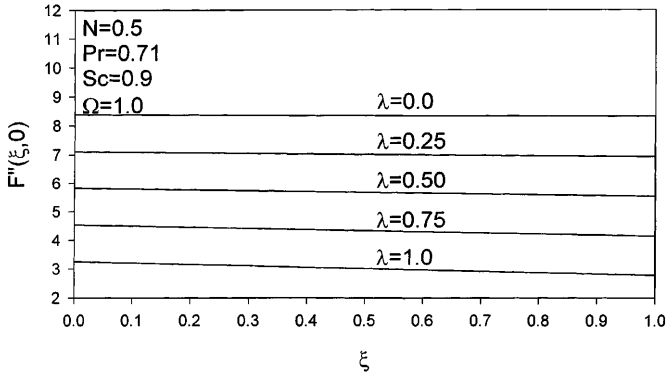

Fig. 23. Effect of λ on the skin friction (UHF/UMF)

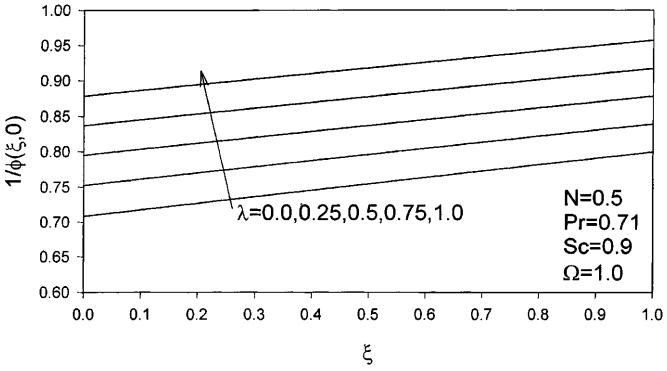

Fig. 24. Effect of λ on the heat transfer (UHF/UMF)

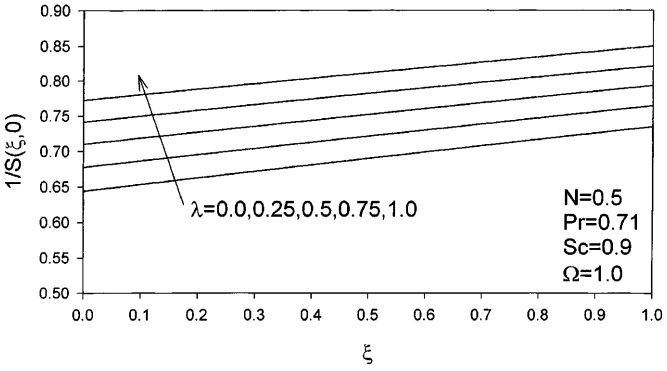

Fig. 25. Effect of λ on the mass transfer (UHF/UMF)

similar to that in the (UWT/UWC) case. Also the skin friction for the (UHF/UMF) case is slightly more than that in the (UWT/UWC) case, but the opposite trend is observed for the heat transfer and the mass transfer.

7 Conclusions

The buoyancy forces cause considerable overshoot in the velocity profiles. The surface skin friction is strongly dependent on the buoyancy forces due to the thermal and mass diffusion, and on the relative velocity between the wall and the free stream. The surface heat transfer and mass transfer strongly depend on the Prandtl number and the Schmidt number, respectively. The surface skin friction is weakly dependent on the surface curvature. The surface skin friction for the uniform heat (mass) flux case is slightly more than that of the uniform wall temperature (concentration) case, but an opposite trend is observed for the surface heat and mass transfer. The surface skin friction increases with the buoyancy forces or with an increase in the relative velocity, but it decreases with increasing Prandtl number or Schmidt number.

References

1. **Chen TS; Mucoglu A** (1975) Buoyancy effects on forced convection along a vertical cylinder. J Heat Transfer 97: 198–203
2. **Mucoglu A; Chen TS** (1976) Buoyancy effects on forced convection along a vertical cylinder with uniform surface heat flux. J Heat Transfer 98: 523–525

3. **Sparrow EM; Quack H; Boerner CJ** (1970) Local nonsimilarity boundary layer solutions. AIAA J 8: 1936–1942
4. **Sparrow EM; Yu HS** (1971) Local non-similarity thermal boundary layer solutions. J Heat Transfer 93: 328–334
5. **Narain JP; Uberoi MS** (1972) Combined forced and free convection heat transfer from vertical thin needles in a uniform stream. Phys Fluids 15: 1879–1882
6. **Mahmood T; Merkin JH** (1988) Mixed convection on a vertical circular cylinder. ZAMP 39: 186–203
7. **Bui MN; Cebeci T** (1985) Combined free and forced convection in vertical slender cylinder. J Heat Transfer 107: 476–478
8. **Lee SL; Chen TS; Armaly BF** (1986) Mixed convection along vertical cylinders and needles. Proc 8th Int Heat Transfer Conf 3: 1425–1432
9. **Lee SL; Chen TS; Armaly BF** (1987) Mixed convection along vertical sylinders and needles with uniform surface heat flux. J Heat Transfer 109: 711–716
10. **Wang TY; Kleinstruver C** (1989) General analysis of steady laminar mixed convection heat transfer on vertical slender cylinders. J Heat Transfer 111: 393–398
11. **Blottner FG** (1970) Finite-difference methods of solution of the boundary layer equations. AIAA J 8: 193–205
12. **Aziz A; Na TY** (1982) Improved pertubation solutions for laminar natural convection on a vertical cylinder. Warme- und- Stoffubertragung 116: 83–87
13. **Shanks D** (1955) Nonlinear transformations of divergent and slowly convergent sequences. J Math Phys 34: 1–42
14. **Karnis J; Pechoc V** (1978) The thermal laminar boundary layer on a continuous cylinder. Int J Heat Mass Transfer 21: 41–47
15. **Na TA** (1979) Computational Methods in Engineering Boundary Value Problems. Academic Press, New York
16. **Whittacker ET; Watson GN** (1963) Modern Analysis. Cambridge University Press, London